

P. Placke
R. Richert
E.W. Fischer

Rheodielectric spectroscopy on heterogeneous polymer systems – electrorheological fluids

Received: 3 April 1995
Accepted: 24 April 1995

P. Placke · R. Richert (✉)
E.W. Fischer
Max-Planck-Institut für Polymerforschung
Ackermannweg 10
55128 Mainz, Germany

Abstract The technique of rheodielectric spectroscopy is used to investigate the dielectric behaviour of electrorheological fluids (ERF) as a function of external electrical DC-field and/or shear rate. Commercial ERF's consisting of mesoscopic polyurethane particles in a silicone oil matrix were studied. The particles contain a salt which leads to strong dipole moments via the Maxwell-Wagner-Polarization (MWP) if subjected to an external electrical field. In an electrical field the dipoles and, concomitantly, the particles motion become correlated leading to the formation of solid-like structures and significant changes in the

viscosity. We demonstrate that dielectric spectroscopy is capable of monitoring the field and shear rate effects in terms of relaxation strength and relaxation time of the MWP. In electrical or shear fields dipole-dipole correlations increase the MWP's relaxation strength, so that we are able to observe structure formation with dielectric spectroscopy, especially the time resolved response of the ERF to changes in the electrical field or the shear rate.

Key words Electrorheological fluids – dielectric spectroscopy – colloidal suspensions

Introduction

Initially Winslow [1] discovered the electrorheological (ER) effect on oil-particle suspensions. The ER phenomenon is typically defined as the fast and reversible change in the viscoelastic properties of suspensions consisting of electrically polarizable particles in a liquid matrix with the application of large electric fields [1–3]. The basis for this effect is that large induced dipoles create electrostatic interactions among the particles which counteract the viscous flow. The extent by which the viscosity increases in an electrical field is strongly dependent on factors like particle volume fraction of the electrorheological fluid (ERF), shear rate or other mechanical stress factors and the geometry of the flow cell [4]. Due to dipole-dipole interactions in the presence of an external field the particles form

pearl chain structures at small particle volume fractions or other solid-like regions at higher concentrations [5]. During the last 50 years the composition of ERF's has been varied in order to overcome problems such as conductivity, abrasiveness and sedimentation [6–8]. Typical applications for ERF's are electrically adjustable mechanical damping devices (shock absorbers) and mechanical connections or switches (clutches) [7].

The research on ERF's of the last decades mostly describes the dependence of particle or liquid properties on the electrorheological effect. In the present work we investigate the dynamics of structure formation as a function of electric field and shear rate employing dielectric spectroscopy. The link between rheological properties of the ERF and its dielectric constants bases on structure formation affecting both the viscosity and correlations among the dipoles which alter the effective dipole moments and thus

the dielectric constant [9]. In this manner we are able to investigate the response of the ERF to the electrical field strength and shear rate faster than by purely mechanical techniques.

Experiment

Sample properties

The commercial electrorheological fluid studied here (Rheobay TP AI 3565, Bayer) [6, 7] consists of polyurethane particles in a silicone oil matrix. The average particle diameter is $d = 5 \mu\text{m}$, their volume fraction in the liquid is about 50%. Salt is added in order to achieve a sufficient conductivity of the particles so that dipoles can be induced by an external electrical field. Before starting an experiment the samples were shaken for several hours and exposed to an ultrasonic bath in order to destroy possible aggregates and sedimentation of the particles. A sample prepared in this manner was used for not longer than 24 hours.

Experimental setup

The apparatus outlined in Fig. 1 is a combination of two independent systems. One is the Bohlin VOR rheometer with its control unit (slave PC) and the second is the dielectric setup with the personal computer (master PC) acquiring the data and controlling the entire experiment. We had to modify the rheometers couette cell consisting of two concentric cylinders (bop and pot) with insulation to facilitate the simultaneous dielectric experiments. The gap between pot ($\varnothing = 15.3 \text{ mm}$) and bop is $400 \mu\text{m}$ wide. Teflon is used to insulate the pot from the ground potential while a macor ceramic separates the bop. This type of measurement cell has the advantage that a constantly rotating pot causes a constant shear rate in the gap and an electrical field is nearly constant as well. Available shear rates $\dot{\gamma}$ are $0\text{--}1600 \text{ s}^{-1}$ for the gap-size of $400 \mu\text{m}$. The bop takes the torque transmitted by a sheared sample. The necessary teflon insulation for the pot reduces heat transmission from the heating bath to the couette cell, however, temperatures from 260 K to 370 K could be achieved. To control the samples temperature exactly, an additional PT100 temperature sensor is mounted in the bop. The time-dependent experiments were carried out at a temperature $T = 55^\circ\text{C}$.

To apply high voltages to the couette cell a Heinzing DC-power supply ($0\text{--}250 \text{ V}$) is used. We designed a special AC/DC-crossway to avoid damage to the LCR-meter

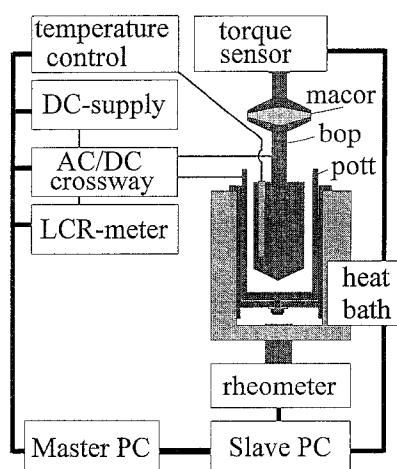


Fig. 1 Schematic setup of the rheodielectric experiment

Genrad 1689 M ($10 \text{ Hz--}100 \text{ kHz}$) caused by high DC-voltages. The necessary AC-voltage (1 V_{rms}) for measuring the dielectric properties is negligible compared to the applied DC-fields. This setup enables mechanical and dielectric spectroscopy on ERF's in large electrical fields ranging from 0 to 625 V/mm , which is sufficient to induce ER-effects. For useful applications of the ER-effect it is necessary to apply stronger electrical fields of the order of kV/mm , but we are limited by the AC/DC-crossways electrical components. Pure mechanical or dielectric spectroscopy was done as well as a combination of both. Time dependent measurements have been done at a single dielectric frequency ($f = 1 \text{ kHz}$) but with different conditions like varying the shear rate or the electrical field strength either continuously or step by step.

Results

The rheological effects of ERF's in electrical fields are well known and presented in Fig. 2 for the ERF Rheobay TP AI 3565. Experimental data can be described by the Bingham model [2] supported by Klingenberg and Zukoski [10, 11], which relates the shear stress τ_M to the quantities yield stress τ_0 , electric field E , shear rate $\dot{\gamma}$, viscosity η , and concentration ϕ .

$$\tau_M(\dot{\gamma}, E, \phi) = \tau_0(E, \dot{\gamma}) + \eta(\phi) \cdot \dot{\gamma} \quad (1)$$

At small shear rates but with application of an electrical field the shear stress τ_M is independent of the shear rate $\dot{\gamma}$. As a function of the electrical field strength the flow curve enters a linear regime at higher shear rates as seen in Fig. 2. The yield stress τ_0 increases with rising electrical field strength according to the power law $\tau_0 \propto E^2$.

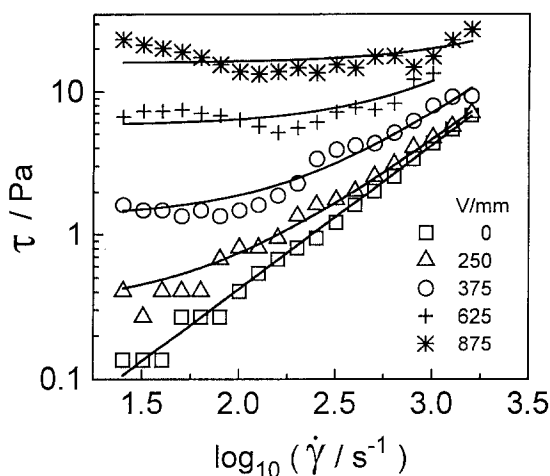


Fig. 2 Dependence of shear stress τ on the shear rate $\dot{\gamma}$ for various electric fields as indicated

The dielectric spectroscopy indicates a strong and temperature dependent relaxation peak which we assign to the Maxwell–Wagner–polarization (MWP) [9, 12–13]. The dielectric data corresponds to a Cole–Cole type function for $\epsilon^*(\omega)$ including a term for the DC-conductivity σ_{DC} :

$$\epsilon^*(\omega) = \epsilon'(\omega) - i\epsilon''(\omega)$$

$$= \epsilon_\infty + \Delta\epsilon(1 + i\omega\tau_D)^{-\alpha} - i\sigma_{DC}/\epsilon_0\omega \quad (2)$$

$$\Delta\epsilon = \epsilon_s - \epsilon_\infty, \text{ with } \epsilon_s = \epsilon'(\omega \rightarrow 0) \text{ and } \epsilon_\infty = \epsilon'(\omega \rightarrow \infty) \quad (3)$$

From fits using Eq. (2) we obtain the characteristic values like relaxation strength $\Delta\epsilon$ and relaxation time τ_D . The exponent α varies only slightly in the range 0.85 to 1, i.e. $\epsilon^*(\omega)$ is close to Debye behaviour. $\Delta\epsilon$ is a measure of the area under the loss function $\epsilon''(\omega)$ and τ_D defines the peak position. Figures 3 and 4 show the dependence of the dielectric loss function $\epsilon''(\omega)$ of the ERF on shear rate $\dot{\gamma}$ and electrical field strength E , respectively.

Since we are in many cases not interested in the absolute amplitudes of the dielectric function or relaxation strength, we normalize the results to the values $\epsilon_n^*(\omega) = \epsilon_n'(\omega) - i\epsilon_n''(\omega)$ which designate the data obtained without shearing and application of a DC field, i.e. for $E = 0, \dot{\gamma} = 0$. The relaxation strength obtained under these conditions is denoted $\Delta\epsilon_n$ and we define

$$K = \Delta\epsilon/\Delta\epsilon_n. \quad (4)$$

The motivation for focusing on the quantity K stems from the notion that the only parameter which should effect $\Delta\epsilon$ at a constant temperature is dipolar correlation which is expected to arise from structural changes in the ERF. We will address this idea in more detail in the Discussion. The $K(E)$ and $K(\dot{\gamma})$ curves corresponding to the results of Figs. 3 and 4 are presented in Figs. 5 and 6, respectively. The

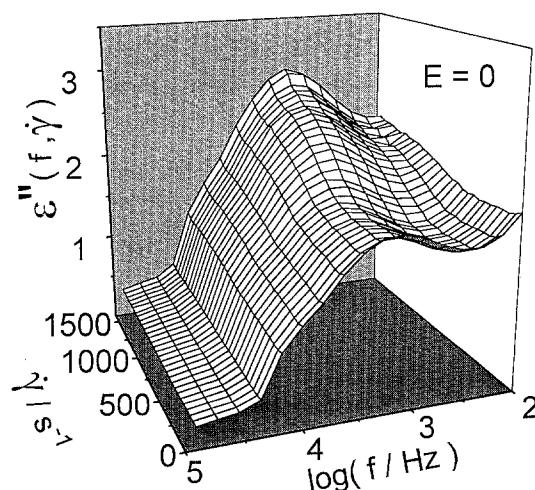


Fig. 3 Dependence of the dielectric loss ϵ'' on the shear rate $\dot{\gamma}$ and frequency f in the absence of a DC-field

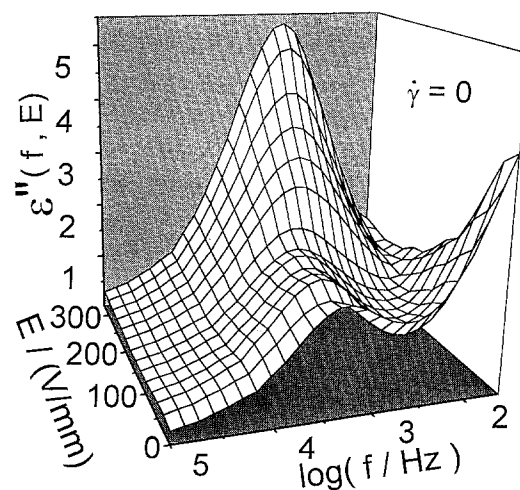


Fig. 4 Dependence of the dielectric loss ϵ'' on the electrical field strength E and frequency f without shearing sample

dependence of the relaxation time τ_D on field strength for the case $\dot{\gamma} = 0$ is shown in Fig. 7.

The value of ϵ'' at a particular frequency ω_0 close to the peak position is nearly proportional to $\Delta\epsilon$, because the increase of $\epsilon''(\omega_0)$ due to an electrical field or a shear rate is much larger than the changes due to τ_D or α of the observed process. We have verified the relation $\epsilon''(\omega_0) \sim \Delta\epsilon$ for several experimental conditions by recording the entire $\epsilon^*(\omega)$ spectra. We can thus use the approximation

$$K \approx \epsilon''(\omega_0)/\epsilon_n''(\omega_0), \quad \omega_0 \approx \tau_D^{-1} \quad (5)$$

for time resolved measurements of K which is faster compared to recording the entire $\epsilon^*(\omega)$ spectra for delineating $\Delta\epsilon$. The following data has been recorded by monitoring

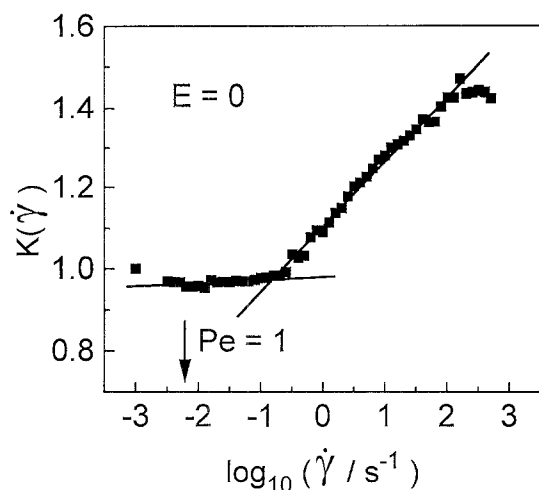


Fig. 5 Dependence of the correlation-factor K on the shear rate $\dot{\gamma}$ for the case $E = 0$. The arrow indicates the position at which the Péclet-number $Pe(\dot{\gamma})$ is unity (see text). Lines serve as guides only

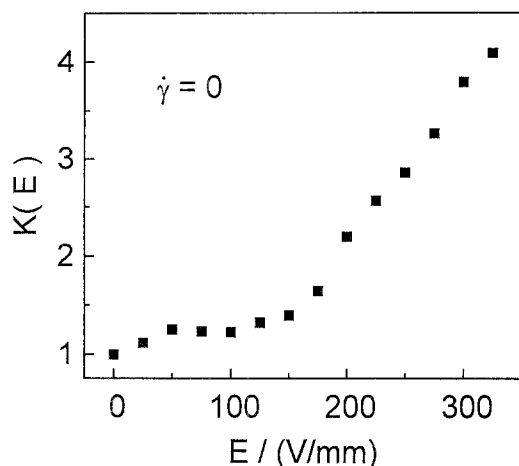


Fig. 6 Dependence of the correlation-factor K on the electrical field strength E for the case $\dot{\gamma} = 0$

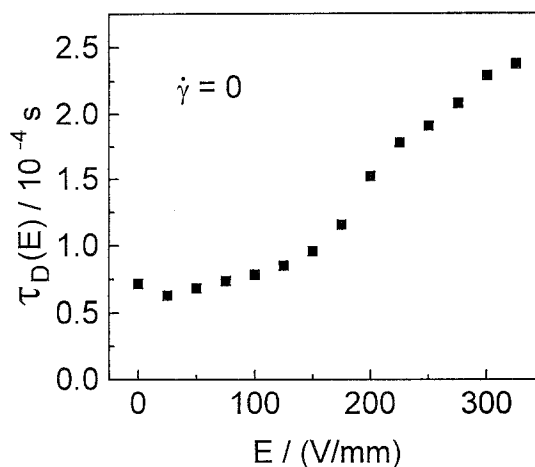


Fig. 7 Dependence of the MWP relaxation time τ_D on the field strength E for the case $\dot{\gamma} = 0$

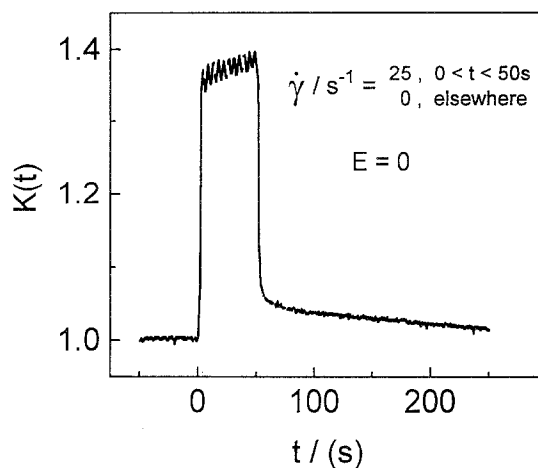


Fig. 8 Effect of switching on and off a shear rate $\dot{\gamma} = 25 \text{ s}^{-1}$ on the correlation-factor K in the case $E = 0$. The slow response time components of K are $\tau_{\text{on}} \approx 50 \text{ s}$ and $\tau_{\text{off}} \approx 130 \text{ s}$

$\varepsilon''(\omega_0)$ as a function of time using $\omega_0/2\pi = 1 \text{ kHz}$, thereby neglecting the minor effects due to $\tau_D(E, \dot{\gamma})$ and $\alpha(E, \dot{\gamma})$ for obtaining $K(t)$.

Figure 8 shows the evolution of $K(t)$ after switching on the shear rate 25 s^{-1} at time $t = 0$ and off again at $t = 50 \text{ s}$. During the first seconds the ERF reacts strongly in terms of K and then slowly approaches higher values of K with a time constant $\tau_{\text{on}} = 48 \text{ s}$. After switching off the shear rate at $t = 50 \text{ s}$ the suspension quickly recovers almost the initial state ($K \approx 1.03$). The relaxation to the initial value $K = 1$ extends beyond the scale of this measurement. Figure 9 displays the response of K to changes of electrical field for the case $\dot{\gamma} = 0$. After applying a field of 250 V/mm

at $t = 0$ the value of K rises suddenly, followed by a minor increase of K with time constant $\tau_{\text{on}} = 13 \text{ s}$. Switching off the field at $t = 50 \text{ s}$ results in two relaxation processes of comparable amplitude but with time scales $\approx 5 \text{ s}$ and $\approx 100 \text{ s}$ i.e. a single exponential function is insufficient for describing the decay in Fig. 9.

Figure 10 shows the result of a similar experiment for $K(t)$ under field switching but while shearing the sample in this case. The most striking difference if compared to Fig. 9 is the much faster recovery of the initial state ($t \leq 0$) after the removal of the field at $t = 50 \text{ s}$. Note also that $K > 1$ for $t \leq 0$ and that K peaks at $t = 0$ instead of at $t = 50 \text{ s}$ as in the $\dot{\gamma} = 0$ case of Fig. 9. The direction of the

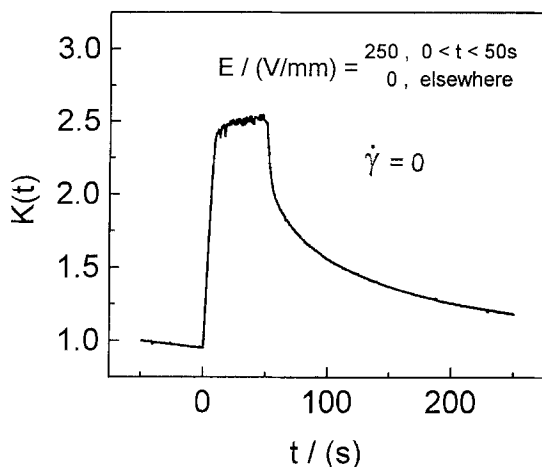


Fig. 9 Response of the correlation-factor K to switching on and off a DC-field of 250 V/mm while switching the field polarity at 1 Hz and without additional shear rate. The resolved components of the response times are $\tau_{\text{on}} \approx 13$ s, $\tau_{\text{off}1} \approx 5$ s and $\tau_{\text{off}2} \approx 60$ s

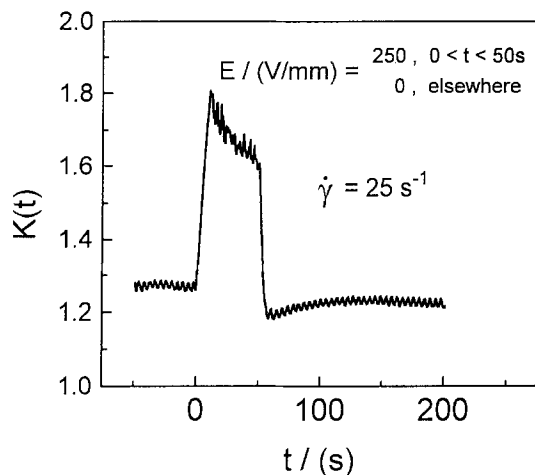


Fig. 10 Response of the correlation-factor K to switching on and off a DC-field of 250 V/mm while switching the field polarity at 1 Hz and with an additional shear rate of $\dot{\gamma} = 25 \text{ s}^{-1}$. The relaxation times of K are $\tau_{\text{on}} \approx 16$ s and $\tau_{\text{off}} \approx 20$ s

(otherwise DC) electrical field was altered every second in order to suppress electrophoresis, which also is responsible for the baseline ripple seen in Fig. 10. Figure 11 shows the same type of experiment but without switching the field direction. When the field is switched on the effects are as strong as presented in Fig. 10 but for $t > 10$ s electrophoresis effects dominate the course of K .

After checking the time dependence of field switching effects on the ERF's behaviour we detected the shear rate dependence at a constant electrical field of 250 V/mm. In

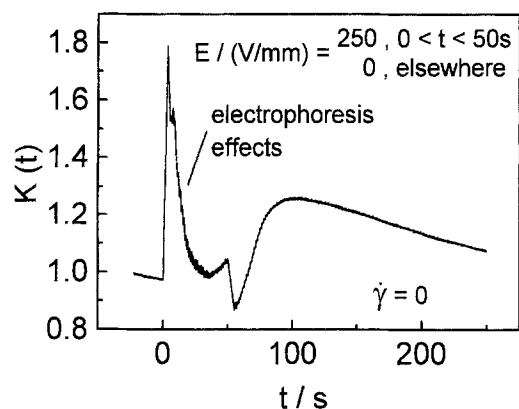


Fig. 11 Response of the correlation-factor K to switching on and off a DC-field of 250 V/mm without switching the field polarity

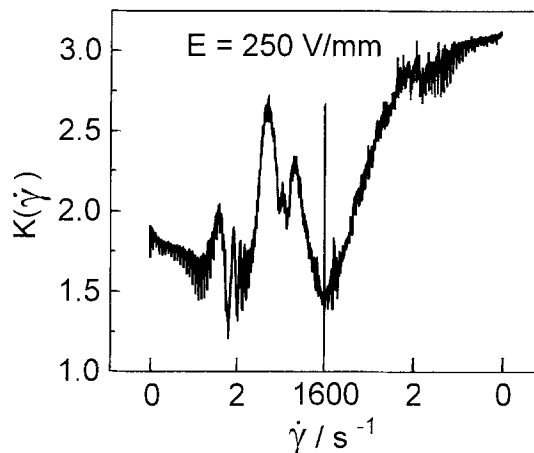


Fig. 12 Dependence of the correlation factor K on shear rate (0 – 1600 s^{-1}) with DC-field of 250 V/mm and polarity switching. Note that the shear rate scale is symmetric with the data subsequently acquired from left to right

the scan shown in Fig. 12 we increased the shear rate from 0 to 1600 s^{-1} followed by a symmetrical decrease back to zero. The highly asymmetric appearance of the $K(\dot{\gamma})$ curve indicates a non-linear behaviour. The data of the left portion of Fig. 12 depends strongly on the scan speed used for increasing the shear rate. Figure 13 illustrates this effect of $K(\dot{\gamma})$ curve parametric in the delay time (10, 30, and 120 s) at each shear rate level. Obviously, the impact of the delay time becomes most pronounced in the low shear rate regime. Such a time dependent behaviour of $K(\dot{\gamma})$ was not observed in the absence of the external electrical field.

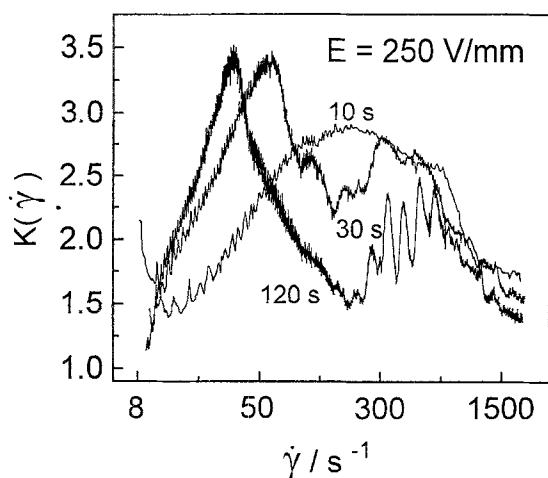


Fig. 13 Dependence of the correlation-factor K on increasing the shear rate from 0–1600 s^{-1} for various delay times (10, 30, and 120 s) before switching to the next higher shear rate value. A DC-field of 250 V/mm with polarity switching is applied in all cases

Discussion

Before interpreting the data we will discuss the significance of the quantity $K = \Delta\epsilon/\Delta\epsilon_n$. In a first order approximation, the relaxation strength $\Delta\epsilon$ of a dielectric is governed by the number density N and a term $\mu^2/3kT$ which depends on the permanent dipole moment μ and temperature according to the Langevin function in the low field limit. In the present heterogeneous system, the dielectric signal stems from the large conductivity of the particles, i.e. field-induced instead of permanent dipoles prevail. The observation that $\Delta\epsilon$ does not depend on the DC-bias voltage at low fields ($E \leq 150$ V/mm) is compatible with the picture that rotational motion of the particles is not involved. In this case one has for small volume fractions ϕ [12, 13]

$$\Delta\epsilon = \epsilon_{sc} - \epsilon_{\infty c} = \epsilon_1(1 + 2\phi)/(1 - \phi) - \epsilon_2(2\epsilon_2 + \epsilon_3 - 2\phi(\epsilon_2 - \epsilon_3))/(2\epsilon_2 + \epsilon_3 + \phi(\epsilon_2 - \epsilon_3)), \quad (6)$$

where $\epsilon_1 = \epsilon_s$, $\epsilon_2 = \epsilon_\infty$ for the silicone and $\epsilon_3 = \epsilon_\infty$ for the particle. $\Delta\epsilon$ refers to the composite and is calculated as difference between static (ϵ_{sc}) and high frequency ($\epsilon_{\infty c}$) dielectric constant.

For a constant value of ϕ it is well known that structural inhomogeneities such as clustering or chain formation leads to enhanced apparent values for $\Delta\epsilon$ or for the effective induced dipole moment [9]. Qualitatively, clustering of the particles strongly increases the polarizability in the vicinity of an induced dipole moment μ , thereby leading to an enhanced reaction field, which in turn in-

creases the effective dipole moment μ^* . Organic solvents of moderate polarity give rise to a ratio $\mu^*/\mu \approx 5$, so that the presently observed range $1 \leq K \propto \mu^*/\mu \leq 3$ appears to be in reasonable agreement with the reaction field effects. Note that the Maxwell–Wagner theory which relates the effective dielectric constants to the DC-conductivities contains no structural information, since the polarizable particle is modeled to be surrounded by dielectric continuum.

Based on the above notions we employ the ‘correlation factor’ K for monitoring changes in structures of the ERF. In the absence of an external field the coulombic repulsion due to the net positive charge of particles counteracts any clustering effects.

It is well known that dipole-dipole interactions are responsible for the rising viscosity of an ERF in an electrical field [3, 10, 14]. The interacting particles stabilize each other and form solid regions. The correlation of particles or dipoles was observed by our experiments leading to a rising yield stress τ_0 (Fig. 2) with increasing the electrical field strength. In parallel we observe a rise of the dielectric relaxation strength $\Delta\epsilon$ with the electric field (Fig. 3).

Shear rate dependence of K

Additionally to the ER-effect in electrical fields we find an increasing correlation in terms of K dependent on the applied shear rate. Due to the net positive charge of the particles and the resulting coulombic repulsion, a configuration with maximum mutual distances will be favoured in the non-sheared fluid. This is a desired effect because repulsion stabilizes the suspension and reduces sedimentation. If the sample is sheared the particles next-neighbour-distances will be forced to fluctuate which results in an inhomogeneous particle distribution in the couette cell. In regions of higher particle density the corresponding correlation-factor K is expected to increase according to the above notions and in agreement with the data of Fig. 5. At shear rates below 0.3 s^{-1} the suspension remains unaffected implying that the mechanical forces are too small to disturb Brownian motion and electrostatic repulsion of the particles. Above an onset shear rates of 0.3 s^{-1} the correlation-factor begins to increase linearly with the shear rate (Fig. 5). This behaviour of a onset followed by a linear regime in terms of the correlation-factor K and maximum position of the MWP time constant τ_D is qualitatively similar to the field induced effect represented by Figs. 6 and 7.

The competition between shear and Brownian forces can be estimated using the dimensionless Péclet-number given by [15]

$$Pe(\dot{\gamma}) = 3\pi\eta_s d^3(\dot{\gamma})/8kT, \quad (7)$$

with the silicone viscosity $\eta_s = 5 \text{ mPa}\cdot\text{s}$, particle diameter $d = 5 \text{ }\mu\text{m}$ and $T = 55^\circ\text{C}$. The balance between shear effects and Brownian diffusion coincides with the condition $Pe(\dot{\gamma}) = 1$, which is achieved at $\dot{\gamma} = 6 \cdot 10^{-3} \text{ s}^{-1}$. This value is well below the onset of shear effects in Fig. 5, indicating that coulombic repulsion dominates over diffusive motion. We conclude that at $\dot{\gamma} = 0.3 \text{ s}^{-1}$ the shear forces start counteracting the repulsion between charged particles.

Figure 8 shows that the sample reacts very quickly if a shear rate is switched on or off, i.e. the particle correlation follows the shear effects immediately. In a couette cell we additionally expect centrifugal forces, which we attribute to the small offset that appears after switching off the shear rate. The particles distribution in the cell thus becomes inhomogeneous not only because of shearing but also because of centrifugal forces which move the particles to the outer wall of the pot. An unambiguous assignment to centrifugal effects is at present not possible.

Electrical field dependence of K

At low electrical fields we find a small yield stress τ_0 leading to only little deviations from a pure Newtonian flow curve. Corresponding to this experiment Fig. 6 shows that in the low field regime the correlation-factor K is field strength invariant. However, above a threshold near $E = 150 \text{ V/mm}$ the correlation-factor increases linearly with E . The time constant τ_D of the MWP also reflects this behaviour (Fig. 7). The straightforward interpretation is that the electric field causes structuring of the particles which affect both the viscosity and dielectric relaxation parameters.

Regarding the response time, Fig. 9 shows that the sample reacts mainly during the first seconds after applying the electrical field at $t = 0$. The response to switching off the field shows that this effect is not symmetric. Compared to the rapid formation of structures at $t = 0$, the suspension relaxes very slowly to its initial state after removing the field. Note that the equilibration process is much slower than that after removing the shear rate (Fig. 8). Obviously, the field induced structures are more stable ($K \approx 2.5$ in Fig. 9) compared to the shear induced case ($K \approx 1.4$ in Fig. 8). In the former case only coulombic repulsion and Brownian motion are responsible for the disappearance of particle clusters, which are stabilized by dipolar interactions. Figure 10 shows the situation of removing the field while constantly shearing the sample, which leads to a significant increase of the speed at which the initial state is restored. A further consequence of shear-

ing the ERF is a relaxation time of $\approx 50 \text{ s}$ needed to establish equilibrium between field and shear induced correlations.

During the experiments related to Figs. 9 and 10 the direction of the electrical field was reversed every second in order to suppress electrophoresis effects. Figure 11 demonstrates the evolution of K under the conditions of the experiments as in Fig. 10, but without altering the sign of E . On comparing the graphs in the time range $0 \leq t \leq 50 \text{ s}$ we conclude that electrophoresis destroys the correlations between the particles within several tens of seconds. The majority of particles move to the anode of the couette cell and eventually a new correlation arises because of the enhanced particle density at the anode. After switching off the field Brownian motion and repulsion destroys the particle layers at the anode.

An interpretation of Figs. 12 and 13 appears in order, where the shear rate is scanned in the range $0 - 1600 \text{ s}^{-1}$ while a constant DC field is applied. The fast oscillations are trivially explained by a slight excentric alignment of bop and pot, which results in oscillating values for $\Delta\epsilon$ at a frequency given by the angular velocity of the cell. Starting at the left of the curve in Fig. 12, $K \approx 1.75$ arises from the electrical field and is maintained up to shear rate values of $\approx 2 \text{ s}^{-1}$. Above this value shearing presumably allows for an improved clustering until at even higher rates the solid like regions are destroyed almost completely, which depresses K significantly above $\approx 150 \text{ s}^{-1}$. The r.h.s. of Fig. 12 indicates a different behaviour upon decreasing the shear rate. A mirror image, which points towards an equilibrium state, is seen only above $\approx 500 \text{ s}^{-1}$. For lower values, K is monotonically increasing while the shearing is attenuated. In this regime, the only effect is lowering the liquids motion which counteracts the structure formation. This asymmetry confirms the idea that switching on a field for a non-sheared sample leads to clusters, which still can be densified further if fluctuations act on the particles. In the low shear regime the ERF's behaviour is thus strongly dependent on the history. The idea is manifested that a medium shear rate equilibrates the particles solid state phase, similar to the effect of thermally induced physical ageing of a glass which has been quenched to well below the glass-transition temperature.

Figure 13 shows three different curves where the shear rate is increased with different delay times of 10 s, 30 s and 120 s between successive steps in $\dot{\gamma}$. Above $\approx 500 \text{ s}^{-1}$ the curves are similar, again implying equilibrium conditions in the high shear regime. At values around 50 s^{-1} a fast scan with only 10 s delay obviously does not allow for the medium shear rate to increase the correlations in terms of K . In other words, the shear induced further densification of clusters proceeds on time scales of the order of 100 s.

Models to describe the ER-effect

For the low shear rate regime the model of Klingenberg and Zukoski rationalizes the phenomenology of ERF's in large electric fields [2, 10, 11, 16, 17]. Highly polarizable particles in a field form dipoles which are aligned strictly parallel to the field direction. As a consequence, attractive forces among the particles results in pearl chain structures or other solid regions. Because of the interaction of the large induced dipoles the viscosity of an ERF increases in electrical fields. If the sample is sheared in this state the pearl chains will be stretched and tilted to the electrical fields direction as long as the shear rate induced mechanical forces do not exceed the electrostatical forces which link the particles. At higher shear rates the pearl chains tear and a region is formed, where the ERF flows. At the border between the solid and the flowing region the mechanical and electrostatical forces are in an equilibrium state. Destroying the solid structures means a decrease of the viscosity and also of the effective dipole moment because the particles are less correlated. If the shear rate (in the couette cell) increases to a level where no solid regions can exist, the viscosity, the dielectric relaxation strength and the correlation-factor K reach a minimum. Due to the high particle concentration at 50% for ERF under study, no pearl chains are formed. However, the phenomenology described by Klingenberg and Zukoski [16] agrees with our observations regarding $K(E, \dot{\gamma})$.

For very high shear rates Block [3] supports the idea that the particles are rotating sufficiently fast, such that their dipoles can no longer interact attractively and the coulombic repulsion gains importance at high shear rates. This effect leads to a decrease of the viscosity and of our correlation factor K . The basis for this effect is the finite time τ_D required to establish the induced dipole moment which depends on the DC-conductivity of the particle. If the particle rotates significantly within the time τ_D the effective field remains zero and no dipole moment is induced. In this case, the field effects and thus the correlation between particles must gradually vanish as the shear rate is increased [3].

Although we do observe a marked decrease of structural correlations at high shear rates, a quantitative estimate indicates that Block's argument does not hold in the present cases. At a maximum shear rate of 1600 s^{-1} the angular velocity of the pot is $\omega = 90 \text{ Hz}$. As an upper

estimate we assume that the particle rotates exactly according to the velocity gradient of the fluid along the particle diameter. The geometrical data for the particle ($5 \mu\text{m } \varnothing$), gap ($400 \mu\text{m}$), and cylinder ($15 \text{ mm } \varnothing$) results in a rotation frequency of the particle of $\approx 500 \text{ Hz}$. This is a factor of ≈ 2 slower than the MWP relaxation time τ_D observed by dielectric spectroscopy. Therefore, Blocks idea cannot explain the decrease of the correlation-factor at shear rates up to 1600 s^{-1} because the induced dipole moment remains almost parallel to the external field at all times.

Conclusions

For a commercial ERF we have employed rheodielectric measurements to investigate the extent and dynamics of field induced structuring, which yields the basis for the electrorheological effects. It has been shown that the easily accessible relaxation strength data reflects structural correlations of the particles in the liquid. The response times of the ERF to changes in the field or shear rate are faster than 1 s, with the exception that field induced structures are stable for $\approx 100 \text{ s}$ in the case of very low shear rates. Based on the time resolved experiments, the field and shear induced structures appear to be different in nature. Additionally, the field induced structures can be densified further by applying moderate shear rates. These above observations imply that the effective state of the ERF is history dependent.

In the low to medium shear rate regime the behaviour of the ERF complies with the model of Klingenberg and Zukoski for describing the formation of solid regions leading to a large yield stress of the liquid within the Bingham model. With increasing the shear rates the solid structures are destroyed and the correlation between particles decreases in the present experimental shear rate and electrical field region. However, this loss of correlation cannot be assigned to a rotational suppression of the induced dipole moments as proposed by Block's model, which should hold only for much larger shear rates.

Acknowledgement We gratefully acknowledge the support of Bayer AG, Leverkusen, Germany, especially Dr. E. Wendt for placing the samples to our disposal and for stimulating discussions.

References

1. Winslow WM (1949) J Appl Phys 20:1137
2. Klingenberg DJ, van Swol F, Zukoski CF (1991) J Chem Phys 94:6170
3. Block H, Kelly JP, Qin A, Watson T (1990) Langmuir 1990:6
4. Atkin RJ, Shi X, Bullough WA (1991) J Rheol 35:1441
5. Chen Y, Sprecher AF, Conrad H (1991) J Appl Phys 70:6796
6. Bloodworth R, Wendt E (1994) Polymer Preprints 35:356

-
7. Bayer AG, Leverkusen (1994) Provisional product information, Bayer Silicone
 8. O'Leary Havelka K (1994) Polymer Preprints 35:315
 9. Böttcher CJF (1973) Theory of electric polarization, Vol 1. Elsevier Amsterdam; Böttcher CJF, Bordewijk P (1978) Theory of electric polarization, Vol 2 Elsevier, Amsterdam
 10. Klingenberg DJ, Zukoski CF, Hill JC (1991) J Chem Phys 73:4644
 11. Klingenberg DJ, van Swol F, Zukoski CF (1989) J Chem Phys 91:7888
 12. Steemann PAM, Maurer FHJ (1992) Colloid Polym Sci 268:315
 13. Hedvig P (1977) Dielectric spectroscopy of polymers Akad Kiadó, Budapest
 14. Jordan TC, Shaw MT, McLeish TCB (1992) J Rheol 36:441
 15. Melrose JR, Heyes DM (1993) J Chem Phys 98:5873
 16. Klingenberg DJ, van Swol F, Zukoski CF (1991) J Chem Phys 94:6160
 17. Klingenberg DJ, Zukoski CF (1990) Langmuir 1990:15